



CrossMark
click for updates

Cite this: *Environ. Sci.: Processes
Impacts*, 2015, 17, 780

Formation of manganese phosphate and manganese carbonate during long-term sorption of Mn^{2+} by viable *Shewanella putrefaciens*: effects of contact time and temperature†

Natalia Chubar,^{*ab} Cristina Avramut^a and Tom Visser^c

The influence of temperature (5, 10, 22 and 30 °C) on the long-term (30 days) sorption of Mn^{2+} by viable *Shewanella putrefaciens* was studied by FTIR and EXAFS. The additional Mn-removal capacity of these bacteria was found to result from the surface precipitation of Mn-containing inorganic phases. The chemical composition of the Mn-containing precipitates is temperature and contact-time dependent. Mn(II) phosphate and Mn(II) carbonate were the two major precipitates formed in 1000 mL batches at 10, 22 and 30 °C. The ratio of Mn(II) phosphate to Mn(II) carbonate was a function of the contact time. After 30 days, $MnCO_3$ was the dominant phase in the precipitates at 10, 22 and 30 °C; however, $MnCO_3$ did not form at 5 °C. Mn(II) phosphate was the only precipitate formed at 5 °C over 30 days. The biosynthesis of Extracellular Polymeric Substances (EPS) was much greater at the lowest temperature (5 °C); however, these polymeric sugars did not contribute to the additional removal of Mn(II) under the experimental conditions. This work is one of the first reports demonstrating the ability of microbes to bioprecipitate manganese phosphate and manganese carbonate. Because of the focus on interfacial processes, this is the first report showing a molecular-level mechanism for manganese carbonate formation (in contrast to the traditionally studied aged minerals).

Received 20th November 2014
Accepted 13th February 2015

DOI: 10.1039/c4em00634h

rsc.li/process-impacts

Environmental impact

The data shown in this work demonstrate that viable *S. putrefaciens* (and most likely some other microorganisms) has a great potential to stabilise (or reduce the mobility in the environment of) Mn^{2+} (and most likely some other metal ions) through processes occurring at the interfaces of the cells for at least 30 days. The interfacial processes start from ion exchange/surface complexation and continue with biomineralisation. Composition of bioprecipitates is a function of temperature, metal loading and bacterial density. The results presented demonstrate that the role of microorganisms in formation of natural minerals might be even greater than thought previously.

Introduction

Microorganisms are well known to play a key role in the cycling of chemical elements in the environment on a global scale, but many molecular-level processes that control such transformations are poorly understood. In 1986, the leading role of bacteria in iron–silica crystalline nucleation was discovered,¹ and the hypothesis that bacteria can be the nucleation sites for

authigenic minerals was proposed one year later² which was confirmed by the same authors.³ Since that time, studies of the roles of microbes in the formation and dissolution of various minerals have resulted in much new knowledge in geochemistry and geology. Manganese attracts special attention from geoscientists because this chemical element forms a variety of precipitates in natural ecosystems, and these precipitates control the cycling of nutrients and xenobiotics in the environment through adsorption, dissolution, and redox transformation processes.^{4–6} Various hydrous oxides of manganese(III, IV) and manganese carbonate ($MnCO_3$) are usually discussed. Less attention has been given to manganese phosphates. Biogenic manganese oxides are highly abundant in the environment.^{7,8} They are reactive and control many redox reactions with organic and inorganic substances. A number of studies have demonstrated that biological Mn(II) oxidation dominates in the environment.^{9,10} Mn-oxides produced by the Mn-oxidising bacteria *Leptothrix discophora*^{11,12} and *Bacillus*

^aUtrecht University, Department of Earth Sciences, Budapestlaan 4, 3584 CD, Utrecht, The Netherlands

^bSchool of Engineering and Built Environment, Glasgow Caledonian University, Cowcaddens Road 70, G4 0BA, Glasgow, UK. E-mail: Natalia.Chubar@gcu.ac.uk; Tel: +44 (0)141 2731779

^cUtrecht University, Department of Inorganic Chemistry and Catalysis, Sorbonnelaan 16, 3584 CA, Utrecht, The Netherlands

† Electronic supplementary information (ESI) available. See DOI: 10.1039/c4em00634h

sp.^{13,14} have been studied extensively. Interesting research has been conducted to isolate new, diverse Mn(II)-oxidising bacteria from deep environments.¹⁵

Manganese carbonate occurs naturally as the mineral rhodochrosite.⁴ Rhodochrosite is rarely in its pure form and primarily forms solid solutions with carbonates of iron, calcium, zinc. Recently, the role of microorganisms in the formation of MnCO₃ was studied using samples of Mn-carbonate ores collected at Adilabad, India,¹⁶ and Sichuan Province, China.¹⁷ Mukhopadhyay¹⁶ concluded that the formation process of Mn-carbonate was induced by microbes and continued through abiotic precipitation and growth of the previously formed crystals. Fan¹⁷ found that Gayan Mn-carbonate ores were rich in organic matter and that microbially induced sulphate reduction played an important role in the formation of these ores during early diagenesis. Manganese phosphates are currently known to be less widely distributed in the environment than manganese carbonates. Manganese phosphates are often solid solutions rich in lithium and iron, Li(Mn, Fe)PO₄, and with other metals (such as Mg, Ca, Al, Zn, K, Cu and others). A manganese phosphate mineral was characterised by Kampf,¹⁸ however, new manganese phosphate species have been discovered by Franolet¹⁹ and recently by Cooper²⁰ what is most likely not the last discovery of new phosphate minerals. Laboratory studies of biogenic precipitation usually address the molecular-level process of the oxidation of redox metals by oxidising microbes (biogenic metal oxides) or use aged minerals (carbonate formation). The role of microorganisms in the formation of manganese carbonates in different regions of the globe has been demonstrated.^{17,21–23} However, only aged manganese carbonate minerals were studied, so (indirect) theoretical conclusions were found instead of experimental evidence. Molecular level research, which would demonstrate the formation process of MnCO₃, has not been conducted to date.

For manganese phosphates, the initial study, which showed that microbes also played an important role in the formation of manganese phosphate minerals, was the recent work by the authors.²⁴ This study resulted from the non-traditional decision to study the sorption of manganese, a redox metal in the reduced state, Mn²⁺, by the reducing bacteria, viable *Shewanella putrefaciens*. The authors discovered the capacity of viable *S. putrefaciens* to sorb Mn²⁺ over 30 days despite the previously unknown ability of these microbes to form Mn-phosphates. To deepen knowledge about the novel processes at the interface of viable cells of *Shewanella putrefaciens* with aqueous Mn²⁺, additional experiments were performed to define the influence of various temperatures (5, 10, 22 and 30 °C) on Mn(II) sorption, on the chemical composition of the Mn-containing precipitates formed and on the formation of EPS. These experiments resulted in a new discovery. Changing the experimental conditions (size of the experimental batches: 125 mL in the previous work and 1000 mL in the latest) allowed discovery of the process of manganese carbonate formation. This formation took place a few days after the experiments started and at a later stage than the formation of manganese phosphates. (Manganese carbonates were not formed in 125 mL batches.) These results, which

differ from those in the previous work,²⁴ are shown in the current work. This paper is the first report showing the molecular level processes of manganese carbonate formation initiated by microbes (in contrast to the previously studied aged minerals); this is also the first work demonstrating how the bioprecipitation process of manganese phosphate can be replaced by the formation of manganese carbonate and is thus the first ever possible explanation of why manganese carbonates are much more widely spread in the environment than manganese phosphates. The role of the temperature on the rate of such processes and the chemical composition of the precipitates has also been demonstrated.

The main tasks of this work were to study the temperature (5, 10, 22 and 30 °C) influence on Mn²⁺ sorption by viable *Shewanella putrefaciens* over one month and to characterise precipitates formed at the interface by EXAFS and FTIR.

Materials and methods

Preparation of bacterial suspensions for experiments

The classical microbiological method was followed to prepare suspensions of the viable *S. putrefaciens* strain 200R for the experiments. First, single colonies were transferred from agar plates of Luria–Bertani (LB) media to liquid LB media (5 g of yeast extract, 10 g of tryptone and 10 g of NaCl in 1 litre); then, they were cultured aerobically at room temperature (22 ± 2 °C) under continuous shaking for 24 hours. The cells (grown in the liquid LB media) were used to inoculate larger bottles of LB medium and were grown for 48 hours. This time was chosen because of the discovery of Haas,²⁵ who showed that surface of *S. putrefaciens* cells is most enriched in functional groups at 48 hours of growth. The cells were harvested and then were pelleted by centrifugation. They were washed five times with 0.1 M NaCl to ensure full removal of LB solution from the cells. The large volumes (500 mL) of pelleted cells (to avoid great loss (in %) from filtration) were used to establish direct correlation between the optical density of the pelleted cells and the dry weight of the bacteria. The suspension was carefully mixed and the optical density (at the wavelength of 660 nm) was promptly recorded. The measurements were repeated five times. A 500 mL sample of the suspension (with a known optical density) was filtered through membrane filters with a pore diameter of 0.2 μm (Advanced Microdevices Pvt. Ltd). The filtered sample was dried at room temperature, and then in an oven at 120 °C. The weight of the dried filter was preliminary measured. This procedure establishes the direct correlation between the optical density of the viable cells and the dry weight of the same cells' biomass (to be used as a unit of measurements of an adsorptive performance). This ratio remains constant in spite of the changes in the cells' viability during the long-term contact of viable cells with aqueous Mn²⁺. The experiments were repeated 5 times. The values measured each time differed from the average value by no more than 10%. The average value of the ratio between the optical density and the dry weight of the microbial cells was used for future experiments. The cells' viability was changing naturally during the experiments from fully viable to (partly) inactivated what

allowed involvement of both viable (1), viable but non-reproducible (2) and inactivated/dead (3) cells in the experimental system. Such experimental conditions allowed closer the laboratory experimental conditions to the conditions in real environment where all three (known) states of microbes (viable, non-reproducible and dead) coexist. In the same time the unit of measurement of adsorption science (mg of dry weight per litre) was maintained.

Sorption experiments

The batch adsorption investigations were performed with 1000 mL of the bacterial suspension with a density (or adsorbent dose) of $2 \text{ g}_{\text{dw}} \text{ L}^{-1}$. It is the traditional adsorbent dose over the last decades as often within its range between 1 and $5 \text{ g}_{\text{dw}} \text{ L}^{-1}$, the adsorptive performance (measured in $\text{mg g}_{\text{dw}}^{-1}$) is the same or very close. The Mn^{2+} concentration was 200 mg L^{-1} . Bacterial suspensions in 0.1 M NaCl were first brought to the necessary temperature (5, 10, 22, and $30 \text{ }^\circ\text{C}$). A pre-set amount of Mn^{2+} (as $\text{MnCl}_2 \cdot 6\text{H}_2\text{O}$) was added to bring the concentration of the cells to $2 \text{ g}_{\text{dw}} \text{ L}^{-1}$ and to pre-set the concentration of Mn^{2+} . No nutrients except for the background electrolyte, 0.1 M NaCl added initially, were provided to the microbes during the sorption experiments. The exact concentration of the bacterial cells was analysed before and after the addition of Mn^{2+} . The large glass beakers containing the microbial suspension were covered with caps to protect the microbial culture from contamination. The caps were removed (opened) once a day for a few minutes to take small samples for analysis. The kinetics of Mn(II) uptake were regularly studied, but the “adsorbent” samples for the spectroscopic analyses were taken at the end of the experiments (at 30 days). We avoided frequent sampling (on a daily basis) of the “adsorbent” from the experimental batches to maintain the same experimental conditions as the kinetics studies. A few additional ambient and $30 \text{ }^\circ\text{C}$ temperature experiments were performed to collect samples after less than 30 days (in 6, 9 and 10 days) at an initial concentration of Mn^{2+} of 200 mg L^{-1} . The samples were centrifuged, were filtered with a $0.2 \text{ }\mu\text{m}$ pore diameter filter (Advance Microdevices P. Ltd) and were carefully dried at ambient temperature for the spectroscopic investigations.

Fourier transform infrared (FTIR) spectroscopy

The FTIR spectra of the air-dried samples of bacteria were recorded in KBr pellets at ambient conditions with a Perkin-Elmer 2000 FTIR spectrometer equipped with a DTGS detector.²⁴ The sample compartment was flushed with dry air to reduce interference from H_2O and CO_2 . The optical resolution of the spectra was 4 cm^{-1} , and 25 scans were accumulated for each spectrum.

EXAFS (Extended X-ray Absorption Fine Structure) and XANES (X-ray Absorption Near Edge Structure)

The experimental and reference samples were ground to very fine powders and were mixed with boron nitride, while considering the percentage of Mn in each sample measured from the adsorption experiments. The samples were mounted

in 1 mm-thick sample holders for EXAFS and XANES data collection. The spectra were recorded at the Mn K-edge (6539 eV) in transmission mode at ambient temperature at the Dutch-Belgian beamline (DUBBLE) (BM 26A) of the European Synchrotron Radiation Facilities.²⁶ The monochromator was calibrated by assigning an energy value of 6539 eV to the first inflection point in the absorption edge of a reference foil of Mn. The data were first calibrated to 6539 eV of E_0 . Both the treated and raw data were used for the data analysis. IFFEFIT program components (ATHENA, ARTEMIS, stand-alone ATOMS from the DEMETER) were used to analyse the data through linear combination fitting and principle component analysis.²⁷ Ten (commercially available, see: Chubar²⁴) reference substances ($\text{Mn}_3(\text{PO}_4)_2$, MnCO_3 , MnCl_2 , MnSO_4 , MnO , MnO_2 (powder), MnO_2 (pyrolisite), $\text{MnO}(\text{OH})$ (manganite), Mn_2O_3 , and Mn_3O_4) were recorded at DUBBLE and were used for analysis with the IFFEFIT programs.

Analytical chemistry methods

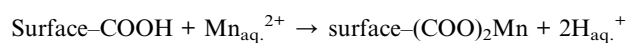
Concentrations of Mn^{2+} was analysed with ICP-OES (inductively coupled plasma optical emission spectrometry). For ICP-OES, SPECTRO CIROS^{CCD} (by SPECTRO Analytical Instruments GmbH – Germany) was applied through the Watertaak2004 method.

Results

Kinetics of Mn(II) sorption at various temperatures

Fig. 1 shows the kinetics of the Mn^{2+} sorption by viable (also referred to here as live) *S. putrefaciens* over 3 minutes (Fig. 1A), 3 hours (Fig. 1C) and 30 days (Fig. 1E). In Fig. 1E, the values begin at 1 day (no data are shown for a few seconds to a few minutes of contact time). Fig. 1 also shows the drift of the pH in the same experimental suspensions over 3 minutes (Fig. 1B), 3 hours (Fig. 1D) and 30 days (Fig. 1F).

There was no distinct temperature (5, 10, 22 and $30 \text{ }^\circ\text{C}$) influence on the Mn^{2+} sorption over 3 hours contact time (Fig. 1C); however, temperature influence was observed over 30 days (Fig. 1E). The rate of Mn(II) removal increased proportionally to temperature. The periods of sharp, fast decreases of Mn^{2+} in the solutions took place on days 7, 12 and 23 at 30, 22 and $10 \text{ }^\circ\text{C}$, respectively; however, those periods were never observed at $5 \text{ }^\circ\text{C}$ over 30 days. The removal of Mn(II) at $5 \text{ }^\circ\text{C}$ was slow and continuous. Despite the absence of a temperature effect on Mn(II) removal over 3 hours, the pH drift in the experimental suspensions (Fig. 1B and D) demonstrated that the interfacial processes occurring at higher (22 and $30 \text{ }^\circ\text{C}$) and lower (5 and $10 \text{ }^\circ\text{C}$) temperatures differed from one another. In the first few minutes, when the living cells came into contact with the metal ions, the pH dropped (from 6.7 to 6.1 and to 5.7) at 22 and $30 \text{ }^\circ\text{C}$ but increased at 5 and $10 \text{ }^\circ\text{C}$ (from 6.7 to 7.0 and to 6.9). Decrease in pH at 22 and $30 \text{ }^\circ\text{C}$ resulted from cation exchange of the surface H^+ for the aqueous Mn^{2+} in accordance with the reaction (using an example of carboxylic functional groups):



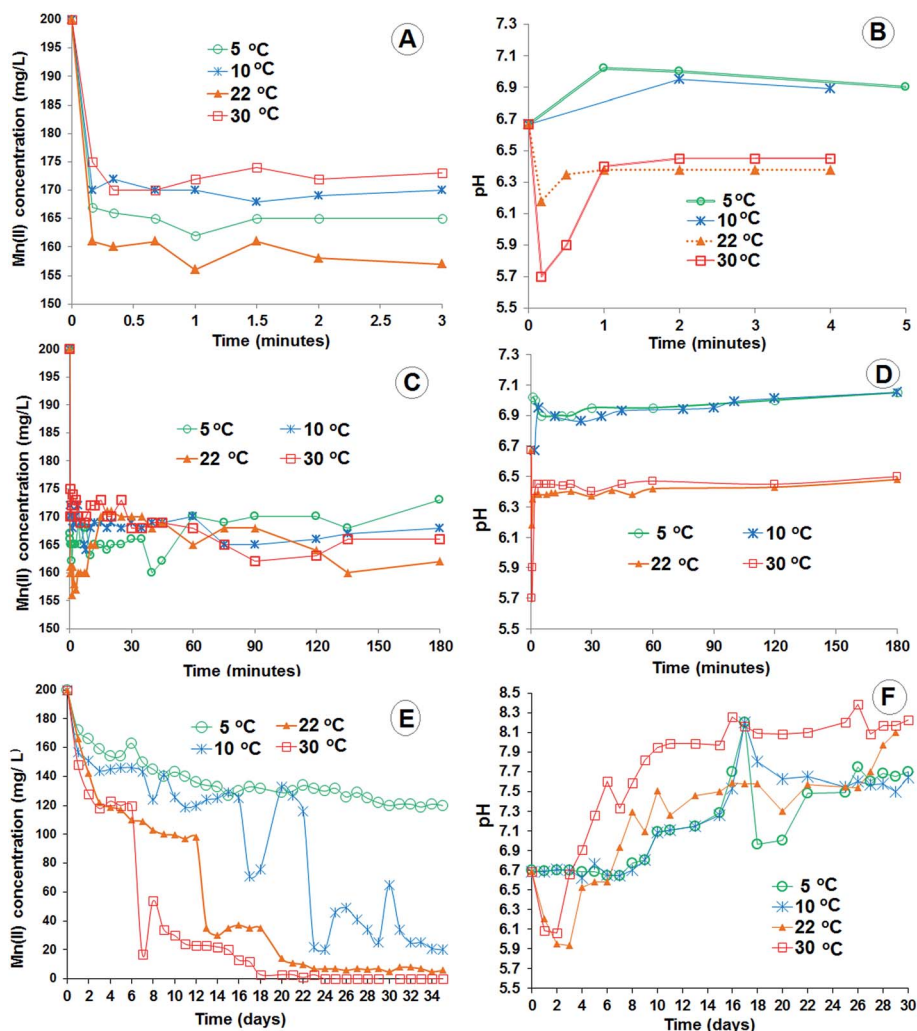


Fig. 1 Kinetics of Mn^{2+} sorption by viable *S. putrefaciens* at 5, 10, 22 and 30 °C over 3 minutes (A), 3 hours (C) and 30 days (E) and the corresponding pH drift (B, D and F). Experimental conditions: bacteria density = $2 \text{ g}_{\text{dw}} \text{ L}^{-1}$, volume of viable bacterial suspensions = 1000 mL, and initial Mn^{2+} concentration = 200 mg L^{-1} .

The physiological pH of these microbes (*i.e.* the pH microbial cells maintain in 0.1 M NaCl with no Mn^{2+} or other metal cations like Cu^{2+} or Zn^{2+} until they are viable >90%) was the same (6.7) at 5, 10, 22 and 30 °C during one week that is an observation from the blank experiments.

At 5 and 10 °C, the viable cells of *S. putrefaciens* re-established the physiological pH (6.7) in 1 day and maintained pH stability over the next 7 days while continuing to slowly sorb Mn^{2+} . At 22 °C, the physiological pH was re-established in 4 days, but the living cells were only able to maintain the pH for 3 days (from days 4 to 6, Fig. 1F); then, the pH increased. At 30 °C, the pH changed on a daily basis (Fig. 1F).

FTIR spectra of *S. putrefaciens* exposed to aqueous Mn^{2+}

Fig. 2 shows the FTIR spectra of *S. putrefaciens* exposed to 200 mg L^{-1} of Mn^{2+} for 30 days at 5, 10, 22 and 30 °C.

Because of the considerable changes in almost all the spectral regions, the spectra are shown in three parts to distinguish

the differences. The spectral region of $1200\text{--}400 \text{ cm}^{-1}$ (Fig. 1A) reflects the largest changes and shows the formation of the two major precipitates (Mn(II) phosphate and Mn(II) carbonate) and the polysaccharides (EPS) produced by the viable cells. The presence of the latter can be concluded from the changes in the bands near 1060 and 580 cm^{-1} .^{28,29} More detailed study of this spectral region shows that the biosynthesis of the polymeric carbohydrates decreases as temperature increases and is practically absent at 30 °C (in 30 days). However, this conclusion is estimated because the intensity and the dominance of the IR bands in an overlapping area depend on the ratio and the concentration of the substances with IR-active bands. Fig. 1E demonstrates that the amount of precipitates formed at 5 °C was much lower than that at other temperatures (10, 22 and 30 °C). In contrast, a large amount of EPS was formed, as is reflected by the broad and intense bands at approximately $1000\text{--}1100$ and $550\text{--}600 \text{ cm}^{-1}$ (Fig. 1A), which indicate the presence of EPS, as demonstrated by our colleagues.^{28,29}

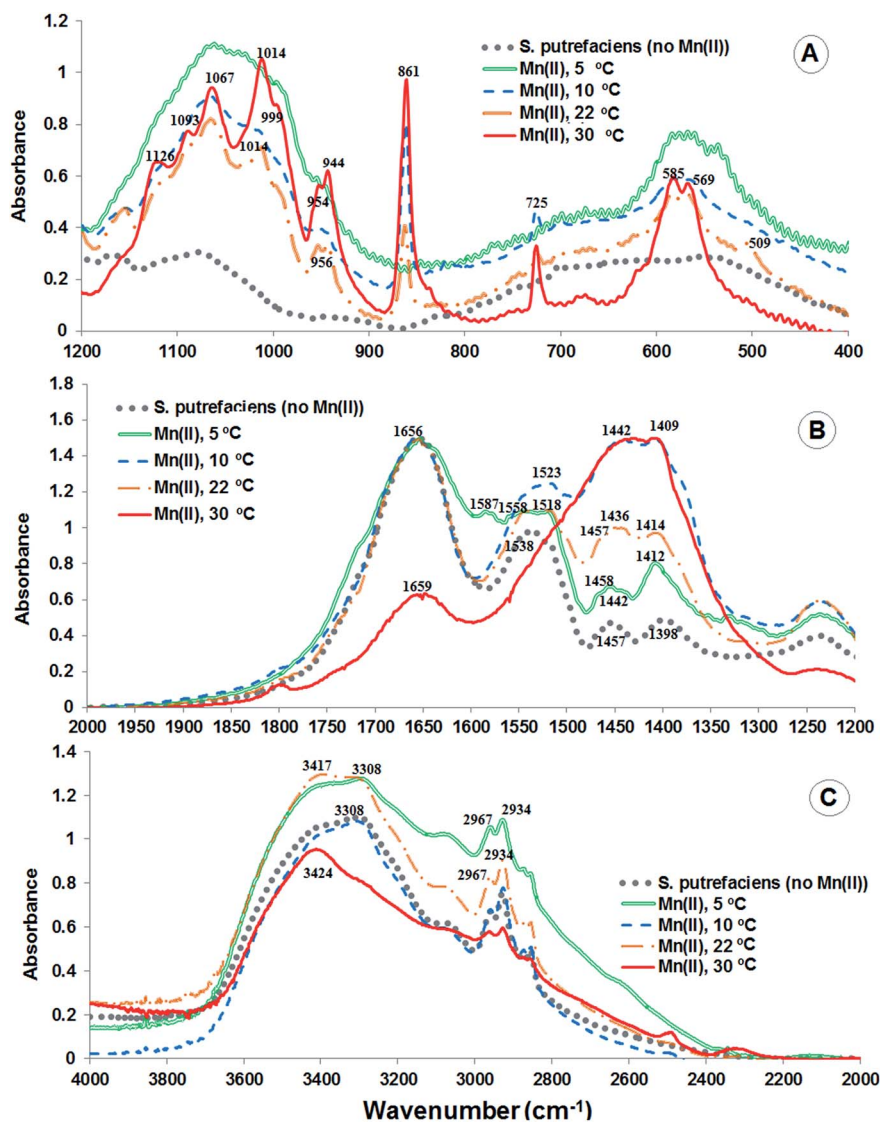


Fig. 2 FTIR spectra of *S. putrefaciens* in contact with aqueous Mn^{2+} at $400\text{--}1300\text{ cm}^{-1}$ (A), $1300\text{--}2000\text{ cm}^{-1}$ (B) and $2000\text{--}4000\text{ cm}^{-1}$ (C). Experimental conditions: temperatures = 5, 10, 22 and 30 °C; contact time = 30 days; $\text{Mn}_{\text{initial}}^{2+} = 200\text{ mg L}^{-1}$; volume of viable bacterial suspension = 1000 mL; and bacteria density = $2\text{ g}_{\text{dw}}\text{ L}^{-1}$.

Because of the overlapping (very intense) carbohydrates bands (which are wider than the bands of the inorganic phases), the formation of Mn(II) phosphate is virtually absent at 5 °C in the FTIR spectra; this absence implies that EXAFS studies are required to confirm the biosynthesis of Mn(II) phosphates at 5 °C. However, the generation of Mn(II) phosphate at 10, 22 and 30 °C is demonstrated by the similarity of the bands near 1060, 1010, 942 and 580 cm^{-1} in the sample data (Fig. 2A) and in the reference spectrum of this compound (Fig. 1SA, ESI†). In contrast, the intensity increase in the bands is not proportional because manganese phosphate was not an individual substance; it was one of the constituents in the mixture (microbial biomass, Mn-phosphate and Mn-carbonate) that formed stepwise over a month. The recently formed manganese phosphate most likely interacted with the other particles and molecules as is reflected by the different ratios of the characteristic bands of manganese phosphate in Fig. 2A. However,

these characteristic bands of Mn(II) phosphate were the most distinct (sharp) at 22 and especially 30 °C. They were less prominent at 10 °C and were almost invisible at 5 °C because of the overlapping bands from the polymeric carbohydrates formed, called EPS. The broad diffuse bands at $1000\text{--}1100$ and $550\text{--}600\text{ cm}^{-1}$ in the FTIR spectrum of the 5 °C sample are so distinct that it is difficult to doubt that a large amount of polymeric carbohydrates is produced by these species at 5 °C.^{28,30} In addition, as illustrated by the spectrum of the 30 °C sample, the band near 580 cm^{-1} grows relatively quickly. This phenomenon can be explained by promotion of the formation of Mn(II) phosphate. Finally, the IR data in Fig. 2A also show the appearance of sharp bands at 861 and 725 cm^{-1} in the FTIR spectra of the three higher temperature samples. These bands perfectly match with those of the reference spectrum of MnCO_3 (Fig. 1SB†). The presence of this compound is additionally confirmed by the large intensity increase in the band near

1433 cm^{-1} (1409, 1442 cm^{-1}) in Fig. 2B. Hence, it is concluded that MnCO_3 formed at higher temperatures (10, 22 and 30 $^\circ\text{C}$) but not at 5 $^\circ\text{C}$. The intensity of the characteristic bands of MnCO_3 (861, 725, near 1433 cm^{-1}) was much lower at 10 $^\circ\text{C}$; this difference demonstrates that the least MnCO_3 formed at this temperature. Further analysis of the spectral region from 2000–1200 cm^{-1} (Fig. 2B) reveals considerable changes in the region from 1600–1500 cm^{-1} , where the amide-II bands are found.³⁰ The spectrum of the 5 $^\circ\text{C}$ sample, for instance, shows a small band near 1587 cm^{-1} , which is absent in the other samples. This band is additional important evidence of the formation of large amounts of EPS.²⁸ Additionally, the amide-II band near 1533 cm^{-1} changes shape and position at higher temperatures. We assume that the observed differences are caused by conformational changes in the peptide chain. Shifts in the bands assigned to the carboxylic stretching modes (1398 and 1457 cm^{-1} in the spectrum of *S. putrefaciens* not in contact with Mn^{2+}) were only observed for the 5 $^\circ\text{C}$ sample. These shifts are evidence that metal complexation to these functional groups was the primary mechanism of Mn^{2+} sorption at the lowest temperature, in contrast to the experiments at 22 and 30 $^\circ\text{C}$ in which manganese(II) removal took place through ion exchange (on H^+), as reflected by the pH drift in Fig. 1B, D and F. The band at 1398 cm^{-1} shifted to 1412 and 1414 cm^{-1} , the band at 1457 cm^{-1} broadened, and additional bands appeared at 1442 and 1436 cm^{-1} in the samples exposed to $\text{Mn}(\text{II})$ at 5 and 10 $^\circ\text{C}$. The largest changes in the spectral region from 4000–2000 cm^{-1} (Fig. 2C) are the decrease in the intensity of the amide N–H stretching band (3100–3500 cm^{-1}) at higher temperatures and the decreased intensity of the C–H stretching bands near 2934 cm^{-1} of the C–H and OH bends, e.g., polymeric sugars. In our opinion, both phenomena are additional evidence that the formation of polysaccharides is suppressed at higher temperature. The spectra of *S. putrefaciens* (without contact with Mn^{2+}) and the sample from the 10 $^\circ\text{C}$ sorption experiments were practically the same in this region, and in our opinion, this similarity confirms that 10 $^\circ\text{C}$ is the most comfortable temperature for these microbes. The latest finding is not novel and is in the agreement with the well-known thriving of these species at low temperatures.³¹

XANES

Fig. 3 shows the XANES (Mn K-edge) of *S. putrefaciens* exposed to 200 mg L^{-1} of Mn^{2+} at 5, 10, 22 $^\circ\text{C}$ over 30 days, at 30 $^\circ\text{C}$ – over 10 days, and 5 references: $\text{Mn}_3(\text{PO}_4)_2$, MnCO_3 , MnO , MnOOH and MnO_2 . XANES examination showed that the manganese was divalent in all samples. (No EXAFS spectrum was collected at 30 days for the 30 $^\circ\text{C}$ sample. The sample was lost.) The inflection point of the absorption edge in the three *S. putrefaciens* samples is at approximately 6542 eV and is evidence of $\text{Mn}(\text{II})$ species.³² For comparison, the (experimental) XANES spectra of trivalent and tetravalent Mn in the reference substances MnOOH and MnO_2 , respectively, are shown in Fig. 3. The inflection point of the absorption edge in these reference samples are at approximately 6545 and 6547 eV, respectively. The shape of the XANES spectra indicates that the

Mn-containing bioprecipitates formed at the interface of the *S. putrefaciens* cells are not hydrous oxides. It is obvious that manganese phosphate and manganese carbonates are the two major precipitates. $\text{Mn}_3(\text{PO}_4)_2$ might be the only precipitate in the 5 $^\circ\text{C}$ sample whereas MnCO_3 is the dominant precipitate in the 10, 22 and 30 $^\circ\text{C}$ samples. The ΔE values for the all experimental samples shown in Fig. 3 were calculated to be 8.1 eV, Fig. 3. For the references, this value was found to be 8.3, 8.8, 10.1, 8.6, and 17.7 eV respectively for $\text{Mn}_3(\text{PO}_4)_2$, MnCO_3 , MnO , MnOOH and MnO_2 . ΔE value for the two 30 $^\circ\text{C}$ samples at 6 and 10 days were calculated to be 8.3 eV.

EXAFS of the samples at 30 days: 5, 10 and 22 $^\circ\text{C}$

The results from examination of the Mn K-edge EXAFS spectra for the three 30 day samples (5, 10 and 22 $^\circ\text{C}$) are shown in Fig. 4A–C as the XANES linear combination fit. ESI shows the k^2 - and k^3 -weighted EXAFS spectra and their Fourier transforms, Fig. 2S–4S.†

EXAFS of the 5 $^\circ\text{C}$ sample (Fig. 2S†) did not show the presence of MnCO_3 . Linear combination fitting by the Athena program (Fig. 4A) showed that the only precipitate formed at this temperature was $\text{Mn}_3(\text{PO}_4)_2$. Using any other reference from the list in the experimental section (hydrous oxides and manganese sulphate and chloride) did not change the result of this LCF modelling. Perfect fitting results were achieved for the 10 $^\circ\text{C}$ sample, Fig. 4B. These results confirmed the formation of both precipitates, $\text{Mn}_3(\text{PO}_4)_2$ and MnCO_3 , and the

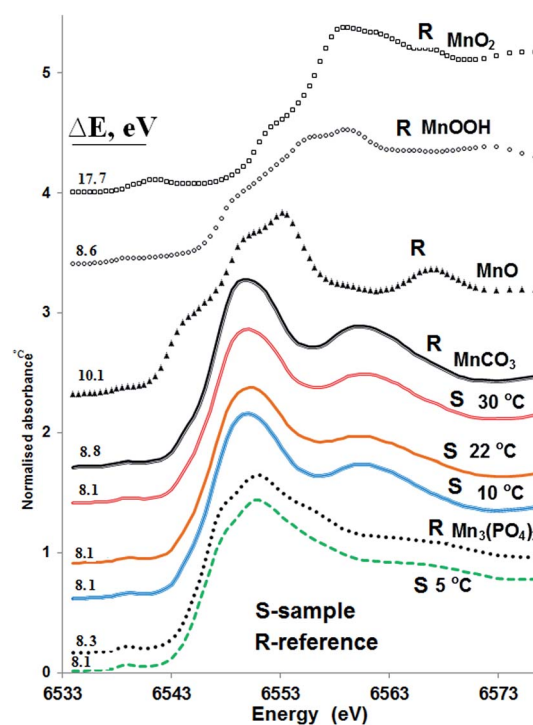


Fig. 3 XANES of Mn-containing samples of *S. putrefaciens* exposed to 200 mg L^{-1} of Mn^{2+} at 5, 10, and 22 $^\circ\text{C}$ over 30 days, and at 30 $^\circ\text{C}$ over 10 days and of the references: $\text{Mn}_3(\text{PO}_4)_2$, MnCO_3 , MnO , MnOOH and MnO_2 .

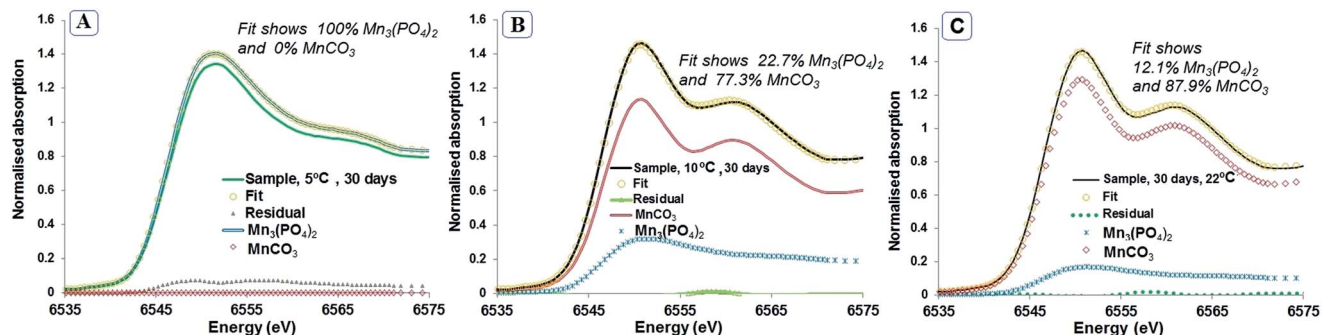


Fig. 4 The XANES linear combination fits of the *S. putrefaciens* samples exposed to Mn^{2+} for 30 days (contact time) at 5 (A), 10 (B) and 22 (C) °C and of the two references ($MnCO_3$ and $Mn_3(PO_4)_2$). Experimental conditions: microbial density = $2\text{ g}_{\text{dw}}\text{ L}^{-1}$, $Mn_{\text{initial}} = 200\text{ mg L}^{-1}$, and volume of viable bacterial suspension = 1000 mL.

predominance of $MnCO_3$ (77.3%). The prevalence of $MnCO_3$ in the composition of the precipitates is also obvious from the plots of the k^2 -weighted EXAFS and the radial structure around the Mn atom (Fig. 3S[†]) of the 10 °C sample with the two references: $Mn_3(PO_4)_2$ and $MnCO_3$. Using EXAFS spectra only, it would be difficult to conclude the presence of manganese phosphate in the 22 ± 2 °C sample as shown by both the k -weighted EXAFS (Fig. 4S[†]) and the radial structure around the Mn atom (Fig. 4S[†]).

This experimental result is an example of the necessity of applying several spectroscopic techniques to complex environmental samples comprising few various phases. The FTIR spectra reflect the bands of manganese phosphate so distinctly (Fig. 2) that it is difficult to doubt the presence of manganese phosphate in the precipitates, Fig. 2. In addition, the Athena program (which is nicely prepared for complex environmental samples with its linear combination fitting option) allowed perfect LCF result to be achieved and concluded that manganese phosphate composes approximately 12.1% of the Mn-containing precipitates formed at ambient temperature in addition to the primary component (87.9%), manganese carbonate (Fig. 4C).

EXAFS of the samples with shorter contact times: time dependence of the formation of the major precipitates

The EXAFS spectra of the few samples collected at less than 30 days were also recorded to observe the temporary changes in the chemical composition of the precipitates formed at 22 and 30 °C. Their linear combination fits are shown in Fig. 5 and 6. Corresponding k^2 - and k^3 -weighted Mn K-edge EXAFS spectra and their FTs are shown Fig. 5S–7S[†]. $MnCO_3$ was found to already be the major precipitate (>50%) at 9 days for an initial Mn^{2+} concentration of 200 mg L^{-1} and at ambient temperature (Fig. 5). The predominance of $MnCO_3$ is also obvious from the comparison of the spectra of *S. putrefaciens* in contact with Mn(II) to those of the references (Fig. 5S and 7S[†]). The percentages of $MnCO_3$ and $Mn_3(PO_4)_2$ precipitated by *S. putrefaciens* on the 9th day as computed by the Athena linear combination fitting model were 64.1 and 33.9%, respectively, Fig. 5. The fitting result was perfect.

Fig. 6 shows the linear combination fitting results for the *S. putrefaciens* samples exposed to Mn^{2+} for 6 (A) and 10 (B) days at 30 °C. We can conclude from Fig. 6S and 7S[†] that $Mn_3(PO_4)_2$ was the major, or possibly the only, precipitate formed by *S. putrefaciens* for exactly 6 days, even at 30 °C. The Athena LCF stated that the percentage of $Mn_3(PO_4)_2$ was still 96.6% (Fig. 6A). The relative content of $MnCO_3$ found by the program's fitting option was 3.4%; however, without any additional spectroscopic data for this sample (such as FTIR) we prefer to limit our conclusions to the statement that the bioprecipitation of $MnCO_3$ begins in 6 days (to avoid giving the exact percentage of this precipitate in the composition). Continuation of the experiment for 4 more days resulted in a completely different ratio of the two major precipitates in the 10 day sample. The percentages of the main two precipitates in the *S. putrefaciens* sample exposed to Mn(II) over 10 days at 30 °C were computed (Athena LCF) to be 29.1% for $Mn_3(PO_4)_2$ and 70.9% for $MnCO_3$, Fig. 6B. Interestingly, these data correlate well with the data for the kinetics of the long-term sorption of Mn(II) (Fig. 1E), which show a plateau in Mn^{2+} sorption from 2 to 6 days followed by a sharp decrease in the Mn(II) concentration in the solution on

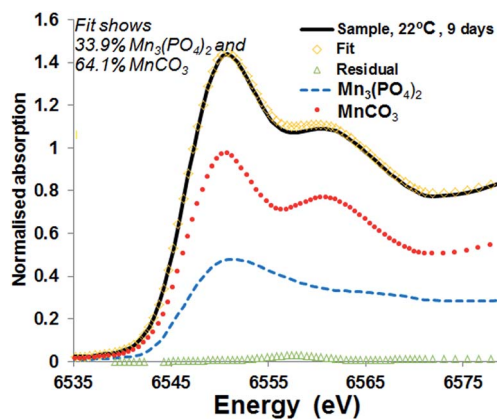


Fig. 5 The XANES linear combination fit of the *S. putrefaciens* samples exposed to Mn^{2+} for 9 days at 22 ± 2 °C and of the two references ($MnCO_3$ and $Mn_3(PO_4)_2$). Experimental conditions: volume of viable bacteria = 1000 mL; bacteria density = $2\text{ g}_{\text{dw}}\text{ L}^{-1}$; and initial Mn^{2+} concentration = 200 mg L^{-1} .

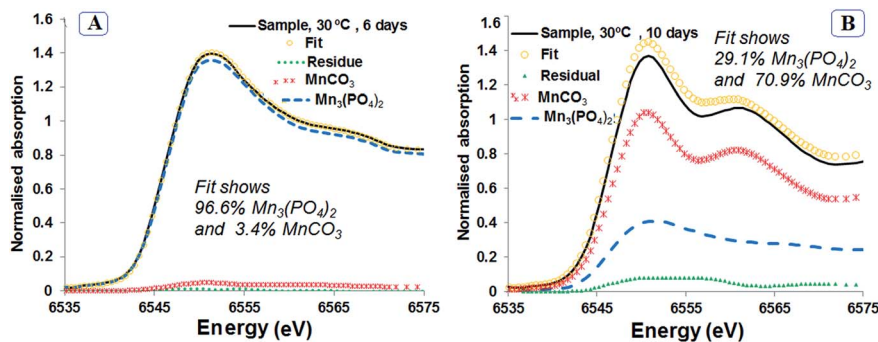


Fig. 6 The XANES linear combination fits of the *S. putrefaciens* samples exposed to Mn^{2+} for 6 (A) and 10 (B) days of contact time at 30 °C and of the two references (MnCO_3 and $\text{Mn}_3(\text{PO}_4)_2$). Experimental conditions: volume of viable bacteria = 1000 mL; bacteria density = 2 $\text{g}_{\text{dw}} \text{L}^{-1}$; and Mn^{2+} initial concentration = 200 mg L^{-1} .

the 7th day. It is easy to conclude that this sharp change in the kinetics curve was caused by the formation of the second precipitate, MnCO_3 .

The rate of generation of MnCO_3 was much faster at the highest temperature (30 °C) than at the other temperatures investigated and followed a regular trend: the higher the temperature, the faster the rate of MnCO_3 formation, Fig. 1E.

Fig. 7 summarises the data for the ratio of the major Mn-containing precipitates formed at the interface with viable *S. putrefaciens* over 30 days at various temperatures (A) and the (available) data for the percentages of the precipitates at higher (22 ± 2 and 30 °C) temperatures and at various contact times. The data at (22 ± 2 and 30 °C) temperatures are plotted together because of the similarities of the interfacial processes at these temperatures reflected by pH drifts (Fig. 1B, D and F).

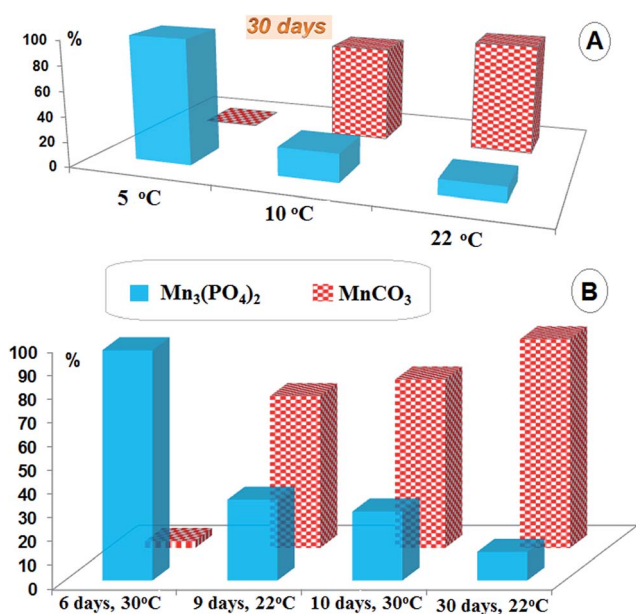


Fig. 7 Ratio of the main Mn-containing precipitates from IFFEFIT linear combination fitting for the samples at 30 days (A) and temporal dependence of the percentages of the major Mn-containing precipitates from the IFFEFIT linear combination fitting at 22 ± 2 and 30 °C (B). Experimental conditions: $\text{Mn}_{(\text{II})\text{initial}} = 200 \text{ mg L}^{-1}$, microbial density = 2 $\text{g}_{\text{dw}} \text{L}^{-1}$, and batch volume = 1000 mL.

The proportion of manganese carbonate in the composition increased as the temperature increased: from zero at 5 °C to 87.9% at 22 ± 2 °C. At the lowest temperature (5 °C) $\text{Mn}_3(\text{PO}_4)_2$ was the only precipitate formed by the microbial species investigated. We can conclude (from Fig. 6A) that there is not clear evidence of the presence of MnCO_3 in the composition of the bioprecipitates (0–3%) on the 6th day; however, on the 9th–10th days the percentage of MnCO_3 was already 64–70% and showed no distinct temperature dependence over this temperature range (22–30 °C), Fig. 5 and 6B. After 30 days, the percentage of MnCO_3 already reached approximately 88%, Fig. 4C.

Discussion

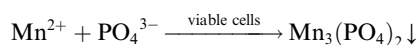
Different mechanism initiating Mn^{2+} sorption by viable *S. putrefaciens* at 5–10 °C and 22–30 °C

The long-term sorption (over 30 days) of Mn^{2+} by the viable gram-negative (Mn(IV), Fe(III) reducing) bacterium *S. putrefaciens* is a complex process that includes a few major stepwise reactions. The interfacial processes begins with ion exchange of H^+ at 22 and 30 °C, which is reflected in the pH decrease (Fig. 1B, D and E); however, a pH decrease was not observed at 5 and 10 °C. Possibly, ion exchange occurs with Na^+/K^+ because of a pH increase at 5 and 10 °C; however, ion exchange is not the dominant process. The difference in adsorption mechanisms at various temperatures (higher, 22 and 30 °C, and lower, 5 and 10 °C) reflected in the pH change demonstrates the strong influence of microbial viability on the interfacial processes. We think that this factor is a function of two variables: concrete microbial species and the affinity of these species to definite aqueous metal cations. The results of similar experiments might not be the same for every microbial species and every metal cation.

We suppose that surface complexation to the functional groups at the bacteria's surface (with no involvement/release of H^+) is the main process occurring in the first few days at the lower temperatures (5, 10 °C). Moreover, the FTIR spectrum of the 5 °C sample shows shifts in the bands assigned to the carboxylic groups (evidence of complexation to these groups) that were not observed at ambient temperatures, Fig. 2B.

Beginning of Mn(II)-bioprecipitation: rate of Mn(II)-phosphate formation as a function of temperature

The bioprecipitation of Mn(II)-containing inorganic phases at the bacterial surface is the continuation of the interfacial reactions that begin 3–4 days after the Mn²⁺ comes into contact with the suspension of *S. putrefaciens*. The process of bioprecipitation always begins with the formation of Mn(II) phosphate at any of the investigated conditions²⁴ and larger batches, various concentrations of Mn²⁺ and various temperatures (5, 10, 22 and 30 °C). This substance remains the major component of the precipitate for more than 1 week at any of the mentioned conditions. The formation of Mn₃(PO₄)₂ can be explained by the release of intracellular inorganic phosphorus and/or protein-like substances (containing phosphate groups) into solutions of the still viable bacteria. Schematic interaction of Mn²⁺ and PO₄³⁻ mediated by viable *S. putrefaciens* can be shown:



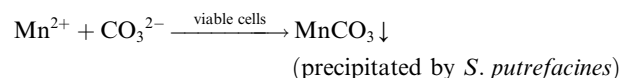
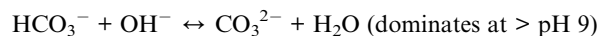
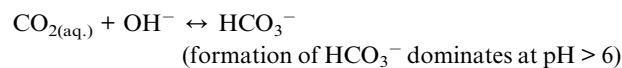
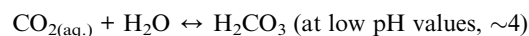
The ability of many microbial species to accumulate inorganic phosphorus intracellularly and to release it under suitable circumstances is a well-known phenomenon.^{33–37} Van Veen³⁷ demonstrated that phosphate uptake through the phosphate inorganic transport system (Pit) is dependent on the presence of divalent cations (such as Mg²⁺, Ca²⁺, Co²⁺, Mn²⁺), which form a soluble, neutral metal phosphate (MeHPO₄); however, the trend for Mn(II)-dependence was not reported. Many Luria–Bertani precursors are prepared with a phosphate buffer. Viable cells of *S. putrefaciens* seemed to accumulate phosphate intracellularly while they grew in the Luria–Bertani solution for two days. They started to release the phosphate within a few days for their physiological needs. The released phosphorus (at lower concentrations) was employed by the same species for the surface precipitation of Mn(II) phosphate. Phosphorus concentration measured in parallel experiments was never higher than 200 mg L⁻¹ as shown in the previous work.²⁴ It ranged 20–120 mg L⁻¹. Within approximately one week, the viability of the living bacteria was depressed (as was demonstrated by few microbiological plate experiments), and the release of phosphate-containing protein-like substances was also decreased. It is possible that the release of the intracellular inorganic phosphorus stopped because of the partial inactivation of viable cells. The absence of inorganic phosphorus release made the formation of Mn(II) phosphate impossible, as was reflected in the absence of Mn(II) removal for a few days, within 2–5 days for the most investigated temperatures (Fig. 1E). However, the partial inactivation of *S. putrefaciens* cells created different physicochemical conditions in the experimental suspensions that allowed MnCO₃ to be formed.

Later stage precipitation: MnCO₃ (≥1 month contact time) only in larger batches and only at higher temperatures (≥10 °C)

MnCO₃ formed in the larger (1000 mL) batches only (in which *S. putrefaciens* was viable for a much longer time than in the smaller (125 mL) batches, as shown in Chubar *et al.* 2013) but only at temperatures ≥ 10 °C. The formation of MnCO₃ did not

start at the same time as the formation of Mn₃(PO₄)₂ but became the dominant process at a later stage. In the first <6 days, Mn₃(PO₄)₂ was still approximately 100%, even for the 30 °C experiment (Fig. 6A), in which the formation of MnCO₃ was the most intense, as was reflected in the fast, sharp decrease of the Mn(II) concentration in the solution (Fig. 1E), and the highest bands of FTIR spectra at 725 and 861 cm⁻¹ assigned to MnCO₃. During the first <6 days, when the formation of Mn₃(PO₄)₂ was the main process (and MnCO₃ was absent), *S. putrefaciens* was at least 60% viable and capable of reproducing. The MnCO₃ process became dominant when (1) most of the bacterial cells no longer appeared viable. The process can be promoted by increasing the pH value (Fig. 1F) and occurs if the concentrations of both Mn²⁺ and carbonate (accumulated through CO₂ uptake) become sufficiently high.

Rise in pH resulted in increase of bicarbonate and carbonate anions (through CO₂ accumulation from air). These anions became available for the interaction with Mn²⁺ and both ions used by bacterial cells to precipitate MnCO₃ in accordance with the schematic reactions:



Until phosphate became available in the solution, the formation of Mn(II) phosphate was the main precipitation process because of the solubility constant of Mn(II) phosphate (log K_s = -27.07)³⁸ compared to MnCO₃ (log K_s = -10.58).³⁹ Concentrations of phosphorous in natural waters, pore solutions of soils and bottom sediments is ≪1 mg L⁻¹.⁴⁰ Concentration of Mn(II) in natural waters is <0.05 mg L⁻¹.⁴¹ Such concentrations of both Mn(II) and phosphate exclude a possibility of Mn phosphate precipitation based on the mineral solubility (without direct or indirect involvement of viable or non-reproducible microbes). As well as manganese phosphate, MnCO₃ could not be formed under the given experimental conditions without microbial activity. In order to synthesise CaCO₃ researchers were continuously bubbling CO₂ into 0.1 mol L⁻¹ CaCl₂ at pH 9.85.⁴² We did not bubble CO₂ into our experimental batches and the flasks were closed (covered by the caps) for >90% of the experiment. pH was not higher than 8.3.

The role of the microbial metabolic activity on the ratio of the main Mn(II)-precipitates at various temperatures (5, 10, 22 and 30 °C) and on the formation of EPS

The processes at the interface of *S. putrefaciens*-Mn²⁺ aqueous at 5 °C were different than those at 10, 22 and 30 °C, and these differences were reflected in the kinetics of the Mn(II) sorption

(Fig. 1A, C and E) and were demonstrated by the FTIR and EXAFS investigations. MnCO_3 did not form after 30 days at 5 °C (Fig. 2 and 4A). $\text{Mn}_3(\text{PO}_4)_2$ was the only precipitate detected by EXAFS (Fig. 4A). We observed that at 5 °C, *S. putrefaciens* cells were viable for a longer time than at the higher temperatures. We do not present quantitative results for the cells' viability. Several tests were performed. They indicated that at all the investigated temperatures, the microbes were at least 60% viable for the first 5 days. It was also obvious (visually) that the microbes became inactivate faster at higher temperatures when their natural pink colour became grey. At 5 °C, the pink colour did not change to grey for almost 2 weeks. In contrast, at 30 °C, the colour became greyish after 6 days. This result means that the stronger metabolic activity of the living cells was an important factor that influenced the processes at the interface. We suppose that if the experiments were continued for longer times, a sharp decrease could be observed for the Mn^{2+} in the solution and the MnCO_3 could be detected later (because of the sharp decrease of the Mn(II) concentration), but this hypothesis must be tested.

We must remark here that the formation of ESP was so intense at 5 °C that it was not possible to detect the Mn(II) phosphates by FTIR alone because of the overlapping bands of from the polymeric sugars (which are wider than the bands for phosphate). We can conclude, however, that the freshly formed ESP did not visibly contribute to the continuation of Mn^{2+} removal from the solution, and this result differs from the literature data on the strong removal capacity of EPS.^{43–45} However this result is similar to those obtained by the other colleagues who reported that the EPS-bearing systems of *Pseudomonas putida* did not enhance the removal of Cd relative to EPS-free system.⁴⁶ It is possible that if we separated the EPS, it could sorb metal ions; however, in the presence of *S. putrefaciens* cells at the higher density of $2 \text{ g}_{\text{dw}} \text{ L}^{-1}$, the processes of Mn(II) phosphate and Mn(II) carbonate bioprecipitation were dominating at the conditions described in this work.

Conclusions

The data shown in this work demonstrate that viable *S. putrefaciens* (and most likely some other microorganisms) has a great potential to stabilise (or reduce the mobility in the environment of) Mn^{2+} (and most likely some other metal ions) through processes occurring at the interfaces of the cells for at least 30 days. After initial contact with Mn^{2+} , the interfacial processes resulted from the bacteria surface chemistry and the role of ion exchange (of H^+) or complexation (with no involvement/release of H^+) depended on the temperature. Several days after the viable cells of *S. putrefaciens* came into contact with the Mn^{2+} , they precipitated a Mn-containing inorganic phase. The chemical composition of the new inorganic phase was greatly dependent on the metabolic activity of the viable microbes, which was, first of all, a function of the temperature, the total amount of cells and the metal loading. Temporary changes in the composition of the new inorganic phase may also depend on the solubility constants of the inorganic precipitates and the availability of the corresponding anions in the solution.

Ion exchange of H^+ was the main process that initiated the processes at the interface of *S. putrefaciens*- Mn^{2+} at 22 and 30 °C; however, at 5 and 10 °C, (probably) because of much stronger hydrogen bonding, metal complexation with the microbial surface functional groups (at least, carboxylic groups) was the initial step. In the 1000 mL batches with a bacteria density of $2 \text{ g}_{\text{dw}} \text{ L}^{-1}$, the two major Mn-containing inorganic phases ($\text{Mn}_3(\text{PO}_4)_2$ and MnCO_3) formed at 10, 22 and 30 °C, but only one main phase ($\text{Mn}_3(\text{PO}_4)_2$) was detected at 5 °C over 30 days. The formation of MnCO_3 started later (after 6 days) when the viable cells no longer provided intracellular inorganic phosphorus and when the pH of the solution became higher.

In the presence of *S. putrefaciens* cells, Extracellular Polymeric Substances (EPS) did not contribute to the Mn^{2+} removal; however, they might sorb manganese(II) ions when preliminarily separated from the bacterial biomass.

Acknowledgements

Financial support under the form of the European Union Marie Curie IIF Fellowship to N. Chubar (grant no. MIF1-CT-2006-021922) and Dutch Ministry of Scientific Research NWO (grant no. 195.068.281) funded the EXAFS/XANES studies at BM26A of ESRF (experiment no. 26-01-794) are gratefully acknowledged. We thank the anonymous reviewers and the editor who helped to improve this work considerably.

References

- 1 F. G. Ferris, T. J. Beveridge and W. S. Fyfe, *Nature*, 1986, **320**, 609–611.
- 2 F. G. Ferris, W. S. Fyfe and T. J. Beveridge, *Chem. Geol.*, 1987, **63**, 225–232.
- 3 F. G. Ferris, C. M. Fratton, J. P. Gerits, S. Schultze-Lam and B. Sherwood Lollar, *Geomicrobiol. J.*, 1995, **13**, 57–67.
- 4 A. H. Reidies, *Manganese Compounds: Ullmann's Encyclopedia of Chemical Technology*, John Wiley, 2007.
- 5 Y. Tang, S. M. Webb, E. R. Estes and C. M. Hansel, *Environ. Sci.: Processes Impacts*, 2014, **16**, 2127–2136.
- 6 *Environmental-microbe metal interaction*, ed. D. L. Lovley, ASC press, Washington DC, 2000.
- 7 J. J. Morgan, Manganese in Natural Waters and Earth's Crust. Its Availability to Organisms, in *Manganese and Its Role in Biological Processes: Metal Ions in Biological Systems*, ed. A. Sigel and H. Sigel, Dekker M, New York, 2000, vol. 27, pp. 1–34.
- 8 J. J. Morgan, *Geochim. Cosmochim. Acta*, 2005, **69**, 35–48.
- 9 B. M. Tebo, J. R. Bargar, B. G. Clement, G. J. Dick, K. J. Murray, D. Parker, R. Verity and S. M. Webb, *Annu. Rev. Earth Planet. Sci.*, 2004, **32**, 287–328.
- 10 D. J. MacDonald, A. J. Findlay, S. M. McAllister, J. M. Barnett, P. Hredzak-Showalter, S. T. Krepeski, S. G. Cone, J. Scott, S. K. Bennett, C. S. Chan, D. Emerson and G. W. Luther III, *Environ. Sci.: Processes Impacts*, 2014, **16**, 2117–2126.
- 11 Y. M. Nelson, L. W. Lion, W. C. Ghorse and M. L. Shuler, *Appl. Environ. Microbiol.*, 1999, **65**, 175–180.
- 12 K. Tazaki, *Clays Clay Miner.*, 1997, **45**, 203–212.

- 13 S. M. Webb, B. M. Tebo and J. R. Bargar, *Am. Mineral.*, 2005, **90**, 1342–1357.
- 14 K. Nealson, *The Manganese-Oxidizing Bacteria*, in *Prokaryotes*, Springer, New York, 2006, ch. 3.1.10, pp. 222–231.
- 15 A. S. Templeton, H. Staudigel and B. M. Tebo, *Geomicrobiol. J.*, 2005, **22**, 127–139.
- 16 J. Mukhopadhyay, J. Gutzmer and N. J. Beukes, *J. Earth Syst. Sci.*, 2005, **114**, 247–257.
- 17 D. Fan, J. Ye, L. Yin and R. Zhang, *Ore Geol. Rev.*, 1999, **15**, 79–93.
- 18 A. R. Kampf and P. B. Moore, *Am. Mineral.*, 1976, **61**, 1241–1248.
- 19 A.-M. Fransolet, M. A. Cooper, P. Cerny, F. C. Hawthorne, R. Chapman and J. D. Grice, *Can. Mineral.*, 2000, **38**, 893–898.
- 20 M. A. Cooper, F. C. Hawthorne and P. Cerny, *Can. Mineral.*, 2009, **47**, 173–180.
- 21 M. Polgári, M. S. Drubina and Z. Szabó, *Bull. Geosci.*, 2004, **79**, 53–61.
- 22 P. M. Okitar and W. C. Shanks, *Chem. Geol.*, 1992, **99**, 139–164.
- 23 D. A. Bazylinski and R. B. Frankel, *Rev. Mineral. Geochem.*, 2003, **54**, 217–247.
- 24 N. Chubar, T. Visser, C. Avramut and H. De Waard, *Geochim. Cosmochim. Acta*, 2013, **100**, 232–250.
- 25 R. J. Haas, *Chem. Geol.*, 2004, **209**, 67–81.
- 26 S. Nikitenko, A. Beale, A. van der Eerden, S. Jacques, U. Leynaud, M. Óbrien, D. Detollenaere, R. Kaptein, B. Weckhuysen and W. Bras, *J. Synchrotron Radiat.*, 2008, **15**, 632–640.
- 27 B. Ravel and M. Newville, *J. Synchrotron Radiat.*, 2005, **12**, 537–541.
- 28 F. François, C. Lombard, J. M. Guigner, P. Soreau, F. Brian-Jaisson, G. Martino, M. Vandervennet, D. Garcia, A. L. Molinier, D. Pignol, J. Peduzzi, S. Zirah and S. Rebuffat, *Appl. Environ. Microbiol.*, 2012, **78**, 1097–1106.
- 29 R. Mikutta, U. Zang, J. Chorover, L. Haumaier and K. Kalbitz, *Geochim. Cosmochim. Acta*, 2011, **75**, 3135–3154.
- 30 G. Socrates, *Infrared Characteristic Group Frequencies*, John Wiley & Sons, New York, 1994.
- 31 H. H. Hau and J. A. Gralnick, *Annu. Rev. Microbiol.*, 2007, **61**, 237–258.
- 32 B. L. Stueben, B. Cantrelle, J. Sneddon and J. N. Beck, *Microchem. J.*, 2004, **76**, 113–120.
- 33 T. Berman and G. W. Skyringt, Phosphorus cycling in aquatic microorganisms studied by phased uptake of ^{33}P and ^{32}P , *Curr. Microbiol.*, 1979, **2**, 47–49.
- 34 H. Ohtake, K. Takahashi and K. Toda, *Water Res.*, 1985, 1587–1594.
- 35 R. E. Blake, J. R. O'Neil and G. A. Garcia, *Am. Mineral.*, 1998, **83**, 1516–1531.
- 36 B. L. Turnet, J. P. Driessen, P. M. Haygarth and I. D. Mckelvie, *Soil Biol. Biochem.*, 2003, **35**, 187–189.
- 37 H. W. Van Veen, T. Abee, G. J. J. Kortstee, W. N. Konings and A. J. B. Zehnder, *Biochemistry*, 1994, **33**, 1766–1770.
- 38 G. Friedl, B. Wehrli and A. Manceau, *Geochim. Cosmochim. Acta*, 1997, **62**, 275–290.
- 39 K. S. Johnson, *Geochim. Cosmochim. Acta*, 1982, **46**, 1805–1809.
- 40 A. O. Fadiran, S. C. Dlamini and A. Mavuso, *Bull. Chem. Soc. Ethiop.*, 2008, **22**, 197–206.
- 41 <http://www.hc-sc.gc.ca/ewh-semt/pubs/water-eau/manganese/index-eng.php>.
- 42 H. Watanabe, Y. Mizuno, T. Endo, X. Wang, M. Fuji and M. Takahashi, *Adv. Powder Technol.*, 2009, **20**, 89–93.
- 43 L. Fang, S. Yang, Q. Huang, A. Xue and P. Cai, *Chem. Geol.*, 2014, **386**, 143–151.
- 44 J. Tourney, B. T. Ngwenya, J. F. W. Mosselmans and M. Magennis, *J. Colloid Interface Sci.*, 2009, **337**, 381–389.
- 45 S. P. de Oliveira Martins, F. N. de Almeida and S. Gomes Ferreira Leite, *Braz. J. Microbiol.*, 2008, **39**, 780–786.
- 46 M. Ueshima, B. R. Ginn, E. A. Haack, J. E. S. Szymanowski and J. B. Fein, *Geochim. Cosmochim. Acta*, 2008, **72**, 5885–5895.